

Effects of ω meson self-coupling on the properties of finite nuclei and neutron stars

Raj Kumar¹, B. K. Agrawal² and Shashi K. Dhiman¹

¹*Department of Physics, H.P. University, Shimla - 171005, India.*

²*Saha Institute of Nuclear Physics, Kolkata - 700064, India.*

Abstract

The effects of ω meson self-coupling (OMSC) on the properties of finite nuclei and neutron stars are investigated within the framework of effective field theory based relativistic mean-field (ERMF) model which includes the contributions from all possible mixed interactions between the scalar-isoscalar (σ), vector-isoscalar (ω) and vector-isovector (ρ) mesons upto the quartic order. For a realistic investigation, several parameter sets corresponding to different values of OMSC are generated by adjusting the remaining parameters of the ERMF model to fit the properties of the finite nuclei. Though, all these parameter sets give equally good fit to the properties of the finite nuclei, only moderate values of OMSC are favored from the “naturalness” point of view. The equation of state for the symmetric nuclear and pure neutron matters resulting from the parameter sets with the moderate values of OMSC are in close agreement with the ones obtained within the Dirac-Brueckner-Hartree-Fock approximation. For such parameter sets the limiting mass for the neutron stars composed of β -stable matter is $\sim 1.9M_{\odot}$. It is found that the direct Urca process can occur in the neutron stars with “canonical” mass of $1.4M_{\odot}$ only for the moderate and higher values of OMSC. Some other interesting properties for the neutron stars are also discussed.

PACS numbers: 21.10.-k, 21.65+f, 24.30.Cz, 21.60.jz, 26.60.+c

I. INTRODUCTION

The concepts of effective field theory (EFT) have provided a modern perspective to the relativistic mean-field models [1, 2, 3]. The EFT based relativistic mean-field (ERMF) models are obtained by expanding the energy density functional in powers of the fields for scalar-isoscalar (σ), vector-isoscalar (ω) and vector-isovector (ρ) mesons and their derivatives upto a given order ν . Thus, a ERMF model includes the contributions from all possible self and mixed interaction terms for σ , ω and ρ mesons in addition to the cubic and quartic self interaction terms for σ meson as present in the conventional quantum hydrodynamic based relativistic mean field models [4, 5]. The parameters (or the expansion coefficients) appearing in the energy density functional are so adjusted that the ERMF results for a set of nuclear observables agree well with the corresponding experimental data. The EFT demands that the adjusted parameters must exhibit “naturalness”, i.e., the values of all the parameters should be roughly of same size when expressed in appropriate dimensionless ratios [6]. The lack of “naturalness” implies that the omitted terms are important. Sometimes not all the terms upto a given order ν are considered which might lead to unnaturalness [1]. It is found in Ref. [3] that the ERMF models containing terms upto order $\nu = 4$ can be satisfactorily applied to study the properties of finite nuclei. The inclusion of next higher order terms improves the fit to the finite nuclear properties only marginally. In Ref. [6] it has been shown that even high density behaviour of the equation of state (EOS) of pure neutron matter and β -stable matter are predominantly controlled by the quartic order ω meson self-coupling (OMSC). The effects of inclusion of higher order terms on the high density behaviour of EOS are found to be only modest to negligible.

There have been several parameterizations [2, 7] of ERMF models containing most of the terms upto the quartic order ($\nu = 4$). These parameter sets are obtained by a fit to the set of experimental data for the properties of a few stable closed shell nuclei. The fitted parameters exhibit “naturalness”. But, some of the nuclear matter properties they yield requires attention; the linear density dependence of the symmetry energy coefficient is strong and the nuclear matter incompressibility coefficient K is either little too low or quite high. The linear density dependence of the symmetry energy coefficient and the nuclear matter incompressibility coefficient should be adjusted to yield reasonably the neutron-skin thickness and the centroid energy of the isoscalar giant monopole resonance, respectively.

The FSUGold parameter set is obtained recently [8, 9] in such a way that they give realistic values for all the properties normally associated with the nuclear matter at the saturation density. However, some of the parameters of FSUGold set show deviation from “naturalness”. This may be pointing to the fact that the contributions due to the mixed interaction terms involving $\sigma - \omega$ and $\sigma - \rho$ mesons omitted from the FSUGold parametrization are important. For FSUGold parameters, the limiting mass of the neutron star is only $1.7M_{\odot}$ which might reduce further with the inclusion of hyperons degree of freedom [10, 11]. On the other hand, an early study using ERMF model shows Ref.[6] that by changing the value of OMSC within a reasonable range, the limiting mass of neutron stars can be varied from $1.8M_{\odot}$ - $2.8M_{\odot}$ for a fixed set of nuclear matter properties. Of course, for a realistic variation in the value of limiting mass, the nuclear matter properties must be determined from the experimental data on the finite nuclei. It is also to be noted that in Ref.[6] the effects of the mixed interactions were not considered and no constrain was imposed on the density dependence of symmetry energy coefficient.

In the present work we have performed a realistic investigation involving the effects of OMSC on the properties of finite nuclei and neutron stars using a ERMF model. We consider a ERMF model which includes the contributions from all possible mixed interactions between the σ , ω and ρ mesons upto the quartic order. Like, in the case of FSUGold parametrization, we determine all the properties normally associated with nuclear matter from the experimental data on the finite nuclei. We generate several parameter sets for fixed values of OMSC by adjusting the remaining parameters of the ERMF model to fit exactly the same set of experimental data for the total binding energies and charge rms radii for some closed shell nuclei. The binding energy data is considered for nuclei ranging from normal to the exotic ones. We also include in our fit the value of the neutron-skin thickness for ^{208}Pb nucleus to constrain the linear density dependence of the symmetry energy coefficient. We restrict the value of the nuclear matter incompressibility coefficient to be within $220 - 240$ MeV as required by the experimental data on the centroid energies for the isoscalar giant monopole resonance. The best fit parameters are searched using the simulated annealing method (SAM) which we have applied recently [12, 13] to determine the parameters of the standard and generalized Skyrme type effective forces.

In Sec. II we discuss ERMF model in brief. In Sec. III we discuss the simulated annealing method used in the present work to search for the best fit parameters. Several parameter

sets for the different values of the OMSC generated in the present work are given in Sec. IV. In Secs. V - VII we discuss our results for the symmetric nuclear matter, pure neutron matter, finite nuclei and neutron stars obtained using our newly generated parameter sets and compare them with the ones for the FSUGold parametrization. As a customary, we also compare our results with those obtained using most popularly used NL3 parameter set [14]. Finally, in Sec. VIII we summarize our main conclusions.

II. ENERGY DENSITY FUNCTIONAL

The derivations of the EFT motivated effective Lagrangian and corresponding energy density functionals are well documented in Refs. [1, 2, 3]. In this section we shall outline very briefly the final expressions for the energy density functional and field equations within the mean-field approximations as used in our numerical calculations. The energy density functional containing all the self and mixed interaction terms for the σ , ω and ρ mesons upto the quartic order reads as [2, 6],

$$\begin{aligned} \mathcal{E}(r) = & \sum_{\mu} \phi_{\mu}^{\dagger} \left\{ -i\alpha \cdot \nabla + \beta [M - \Phi(r)] + W(r) + \frac{1}{2}\tau_3 R(r) + \frac{1+\tau_3}{2}A(r) \right\} \phi_{\mu}(r) \\ & + \frac{1}{2} \frac{m_{\sigma}^2}{g_{\sigma}^2} \Phi^2(r) + \frac{\bar{\kappa}}{6} \Phi^3(r) + \frac{\bar{\lambda}}{24} \Phi^4(r) - \frac{\zeta}{24} W^4(r) - \frac{\xi}{24} R^4(r) + \frac{1}{2g_{\sigma}^2} [\nabla \Phi(r)]^2 \\ & - \frac{1}{2g_{\omega}^2} [\nabla W(r)]^2 - \frac{1}{2} \frac{m_{\omega}^2}{g_{\omega}^2} W^2(r) - \bar{\alpha}_1 \Phi(r) W^2(r) - \frac{1}{2} \bar{\alpha}'_1 \Phi^2(r) W^2(r) - \frac{1}{2} \frac{m_{\rho}^2}{g_{\rho}^2} R^2(r) \\ & - \frac{1}{2g_{\rho}^2} [\nabla R(r)]^2 + \bar{\alpha}_2 \Phi(r) R^2(r) - \frac{1}{2} \bar{\alpha}'_2 \Phi^2(r) R^2(r) - \frac{1}{2} \bar{\alpha}'_3 W^2(r) R^2(r) \\ & - \frac{1}{2e^2} [\nabla A(r)]^2 \end{aligned} \quad (1)$$

where, the index μ runs over all occupied states of the positive energy spectrum. The variables Φ , W and R represent the σ , ω and ρ meson fields, respectively, and A is the photon field. We must emphasize at this point that in the present work we consider all the mixed interaction terms.

The mean-field equations for the nucleons, mesons and photons are as follows,

$$\left\{ -i\alpha \cdot \nabla + \beta [M - \Phi(r)] + W(r) + \frac{1}{2}\tau_3 R(r) + \frac{1+\tau_3}{2}A(r) \right\} \phi_{\mu}(r) = \epsilon_{\mu} \phi_{\mu}(r), \quad (2)$$

$$\begin{aligned}
-\Delta\Phi(r) + m_\sigma^2\Phi(r) &= g_\sigma^2\rho_s(r) - \frac{\bar{\kappa}}{2}\Phi^2(r) - \frac{\bar{\lambda}}{6}\Phi^3(r) + \bar{\alpha}_1 W^2(r) \\
&+ \bar{\alpha}'_1\Phi(r)W^2(r) + \bar{\alpha}_2 R^2(r) + \bar{\alpha}'_2\Phi(r)R^2(r),
\end{aligned} \tag{3}$$

$$\begin{aligned}
-\Delta W(r) + m_\omega^2 W(r) &= g_\omega^2\rho(r) - \frac{\zeta}{6}W^3(r) - 2\bar{\alpha}_1\Phi(r)W(r) \\
&- \bar{\alpha}'_1\Phi^2(r)W(r) - \bar{\alpha}'_3 W(r)R^2(r),
\end{aligned} \tag{4}$$

$$\begin{aligned}
-\Delta R(r) + m_\rho^2 R(r) &= \frac{1}{2}g_\rho^2\rho_3(r) - \frac{\xi}{6}R^3(r) - 2\bar{\alpha}_2\Phi(r)R(r) \\
&- \bar{\alpha}'_2\Phi^2(r)R(r) - \bar{\alpha}'_3 R(r)W^2(r),
\end{aligned} \tag{5}$$

$$-\Delta A(r) = e^2\rho_p(r). \tag{6}$$

The different kinds of baryon densities ρ_s (scalar), ρ (total), ρ_3 (isovector) and ρ_p (proton) appearing in Eqs. (3) - (6) are given by,

$$\rho_s(r) = \sum_\mu \phi_\mu^\dagger(r)\beta\phi_\mu(r), \tag{7}$$

$$\rho(r) = \sum_\mu \phi_\mu^\dagger(r)\phi_\mu(r), \tag{8}$$

$$\rho_3(r) = \sum_\mu \phi_\mu^\dagger(r)\tau_3\phi_\mu(r), \tag{9}$$

$$\rho_p(r) = \sum_\mu \phi_\mu^\dagger(r) \left(\frac{1+\tau_3}{2} \right) \phi_\mu(r). \tag{10}$$

The EFT imposes the condition of “naturalness” on the parameters or the expansion coefficients appearing in Eq. (1). The “naturalness” implies that the coefficients of the various terms in the energy density functional, when expressed in appropriate dimensionless ratios, should all be of the same size. The dimensionless ratios are obtained by dividing the Eq. (1) by M^4 and expressing each term in powers of Φ/M , W/M and $2R/M$ [6]. This means that the dimensionless ratios, namely,

$$\begin{aligned}
&\frac{1}{2c_\sigma^2 M^2}, \frac{1}{2c_\omega^2 M^2}, \frac{1}{8c_\rho^2 M^2}, \frac{\bar{\kappa}}{6M}, \frac{\bar{\lambda}}{24}, \\
&\frac{\zeta}{24}, \frac{\xi}{384}, \frac{\bar{\alpha}_1}{M}, \frac{\bar{\alpha}'_1}{2}, \frac{\bar{\alpha}_2}{4M}, \frac{\bar{\alpha}'_2}{8}, \frac{\bar{\alpha}'_3}{8}
\end{aligned} \tag{11}$$

should be roughly of same size. In the above equation $c_i^2 = g_i^2/m_i^2$, where i represents σ , ω and ρ mesons.

III. SAM ALGORITHM FOR χ^2 MINIMIZATION

The SAM is analogous to an annealing process in which a metal, initially at high temperature and disordered, slowly cools so that the system at any time is in a thermodynamic equilibrium. As cooling proceeds, the system becomes more ordered and approaches a frozen ground state at zero temperature. It is an elegant technique for optimization problems of large scale, in particular, where a desired global extremum is hidden among many local extrema. The SAM has been found to be an extremely useful tool for a wide variety of minimization problems of large non-linear systems in many different areas of science (e.g., see Refs. [15, 16, 17]). Recently [18, 19], the SAM was used to generate some initial trial parameter sets for the point coupling variant of the relativistic mean-field model.

In the present work we use SAM to minimize the χ^2 function defined as,

$$\chi^2 = \frac{1}{N_d - N_p} \sum_{i=1}^{N_d} \left(\frac{M_i^{exp} - M_i^{th}}{\sigma_i} \right)^2 \quad (12)$$

where, N_d is the number of experimental data points and N_p the number of fitted parameters. The σ_i stands for theoretical error and M_i^{exp} and M_i^{th} are the experimental and the corresponding theoretical values, respectively, for a given observable. Since, the M_i^{th} in Eq.(12) is calculated using the ERMF model, the values of χ^2 depends on the values of the parameters appearing in Eq. (1). In Ref.[12] we have described in stepwise manner the implementation of the SAM algorithm to determine the best fit parameters for the standard Skyrme type effective forces. To apply SAM one needs to specify the range for each of the parameters needs to be fitted and a set of guess parameters. In Ref. [12] the range of the Skyrme parameters were specified in terms of the properties of the nuclear matter at the saturation density. This was possible, because, the number of the Skyrme parameters to be fitted were directly related to the equal number of nuclear matter properties which led to a drastic reduction in the parameter space so that the best fit parameters could be searched efficiently. For the case of generalized Skyrme type effective forces we used the SAM algorithm by specifying the parameter space directly in terms of the range of each of the parameters [13]. Since, the number of parameters for the generalized Skyrme type effective forces are larger than the number of the quantities normally associated with the nuclear matter. For the ERMF model we have used rather a hybrid approach. The parameters g_σ , g_ω , $\bar{\kappa}$ and $\bar{\lambda}$ of Eq.(1) for a given values of $\bar{\alpha}_1$, $\bar{\alpha}'_1$ and ζ are expressed in terms of the binding energy per

nucleon ϵ , incompressibility coefficient K , effective mass M^* and saturation density ρ_0 for the nuclear matter as follows [1, 20],

$$C_\sigma^2 = \frac{\frac{1}{2}\Phi^2}{\frac{1}{2}\Phi^2 U'' - 3\Phi U' + 6U} \quad (13)$$

$$C_\omega^2 = \frac{W}{\rho - W(2\bar{\alpha}_1\Phi + \bar{\alpha}'_1\Phi^2) - \frac{1}{6}\zeta W^3} \quad (14)$$

$$\bar{\kappa} = \frac{-\Phi^2 U'' + 5\Phi U' - 8U}{\frac{1}{6}\Phi^3} \quad (15)$$

$$\bar{\lambda} = \frac{\frac{1}{2}\Phi^2 U'' - 2\Phi U' + 3U}{\frac{1}{24}\Phi^4} \quad (16)$$

where,

$$\Phi = M - M^* \quad (17)$$

$$W = \epsilon + M - \sqrt{k_F^2 + M^{*2}} \quad (18)$$

$$U' = \rho_s + W^2 [\bar{\alpha}_1 + \bar{\alpha}'_1 \Phi] \quad (19)$$

$$U'' = \rho'_s - l^2 v + \bar{\alpha}'_1 W^2 + \frac{\left(\frac{M^*}{E_F^*} - lv\right)^2}{\frac{\pi^2}{2k_F E_F^*} + v - \frac{K}{9\rho}} \quad (20)$$

with

$$l = -2W (\bar{\alpha}_1 + \bar{\alpha}'_1 \Phi) \quad (21)$$

$$v = \frac{1}{\frac{1}{C_\omega^2} + (2\bar{\alpha}_1 + \bar{\alpha}'_1 \Phi^2) + \frac{1}{2}\zeta W^2} \quad (22)$$

In Eqs. (13) - (22), all the quantities are obtained at the nuclear matter saturation density $\rho = \rho_0$.

In Table I we specify the parameter space in terms of ϵ , K , M^* , ρ_0 and some other parameters. It can be easily verified using second and third columns of Table I that the range of each of the parameters $\bar{\alpha}_1$, $\bar{\alpha}'_1$, $\bar{\alpha}_2$, $\bar{\alpha}'_2$ and $\bar{\alpha}_3$ becomes identical ($0.0 - 2.0 \times 10^{-3}$) when expressed in appropriate dimensionless ratios using Eq.(11). The column labeled “d”

denotes the maximum change allowed in a single step for a randomly selected parameter. The guess values of the parameters which we have used for initiating the SAM are given in last column of Table I. The values of guess parameters are so chosen that they lie in the middle of the specified range. It should be noted that the parameters ζ and ξ denoting the self couplings for ω and ρ mesons do not appear in Table I as they are kept fixed during χ^2 minimization procedure. The best fit parameters for which χ^2 is the minimum are searched within the specified parameter space with the help of annealing schedule. The annealing schedule determines the value of the control parameter $T(k)$ at k -th step starting from its initial value $T(0)$. As in Refs. [12, 13] we use Cauchy annealing schedule given by,

$$T(k) = \frac{T(0)}{k+1} \quad (23)$$

where, starting value of k is equal to zero and is increased in steps of unity after each $100N_p$ reconfigurations or $10N_p$ successful reconfigurations which ever occurs first. We keep on reducing the value of T using Eq. (23) until the efforts to reduce further the value of χ^2 becomes sufficiently discouraging. We have performed test calculations for two different values of $T(0)$ taken to be 2.5 and 5.0. For both the test calculations the final value of the χ^2 function is almost the same. In what follows, we present our results obtained using $T(0) = 5.0$.

IV. NEW PARAMETRIZATIONS OF THE ERMF MODEL

We search for the best fit parameters of the ERMF models by following the χ^2 minimization procedure as briefly outlined in Sec. III. Our data set contains the total binding energies and charge rms radii for several nuclei taken from Refs [21, 22, 23]. We consider total binding energies for $^{16,24}\text{O}$, $^{40,48}\text{Ca}$, $^{56,78}\text{Ni}$, ^{88}Sr , ^{90}Zr , $^{100,116,132}\text{Sn}$ and ^{208}Pb nuclei, charge rms radii for ^{16}O , $^{40,48}\text{Ca}$, ^{56}Ni , ^{88}Sr , ^{90}Zr , ^{116}Sn and ^{208}Pb nuclei. The theoretical error needed to evaluate the χ^2 function (Eq. 12) are taken to be 1.0 MeV for the total binding energies and 0.02 fm for the charge rms radii. In addition, we also fit the value of neutron-skin thickness for ^{208}Pb nucleus to constrain the linear density dependence of symmetry energy coefficient. The very accurate data of neutron-skin thicknesses are still not available. It is shown [24] in a relativistic mean-field based random phase approximation that the neutron-skin thickness of 0.175 fm in ^{208}Pb nucleus and $K \approx 240$ MeV are required

to adequately reproduce the centroid energies of the isoscalar giant monopole and isovector giant dipole resonances. A Dirac-Brueckner-Hartree-Fock (DBHF) calculation [25] using a realistic potential predicts the value of neutron-skin thickness in ^{208}Pb nucleus to be 0.188 fm. However, recently extracted value of neutron-skin thickness for ^{208}Pb nucleus from the isospin diffusion data lie within $0.16 - 0.24\text{fm}$ indicating large uncertainties [26]. In our fit we use the value of neutron-skin thickness to be $0.18 \pm 0.01\text{ fm}$ for the ^{208}Pb nucleus. To this end, we must point out that for our parametrizations, the center of mass correction to the total binding energy E_{cm} is evaluated within the harmonic oscillator approximation which gives $E_{\text{cm}} = \frac{3}{4}\hbar\omega$ and we take $\hbar\omega = 45A^{-1/3} - 25A^{-2/3}\text{ MeV}$.

The parameters ζ and ξ corresponding to self-couplings for ω and ρ mesons can not be very well constrained by the properties of finite nuclei. These parameters mainly determine the high density behaviour of the EOS. The impact of the parameter ξ is found to be appreciable for pure neutron matter only at very high densities [6]. The seven new parameter sets FSUGZ00, FSUGZ01, ..., FSUGZ06 are generated for fixed values of OMSC parameter $\zeta = 0.00, 0.01, \dots, 0.06$ and keeping $\xi = 0$. All the FSUGZ parametrizations give equally good fit to the properties of the finite nuclei. In Table II we give the values only for FSUGZ00, FSUGZ03 and FSUGZ06 parameter sets. In Table III we present the values of these parameters when expressed in dimensionless ratios using Eq. (11). In Tables II and III we also list the values of the parameters for NL3 [14] and FSUGold [8, 9] sets. It is clear from the Table III that for the case of FSUGold parameter set the $\bar{\alpha}'_3$ is quite large in comparison to the other parameters when expressed in appropriate dimensionless ratios. We notice from Table III that the values of the parameters $\bar{\kappa}$, $\bar{\lambda}$, $\bar{\alpha}_1$ and $\bar{\alpha}'_1$ are strongly correlated with the values of ζ . For smaller ζ , the parameter $\bar{\lambda}$ becomes small and negative which not only gives rise to deviations from the “naturalness” behaviour but also gives instabilities in the EOS at high densities. Whereas, for larger ζ , the values of $\bar{\kappa}$, $\bar{\alpha}_1$ and $\bar{\alpha}'_1$ become smaller and once again show deviations from the “naturalness”. Thus, it appears that a moderate value of $\zeta \sim 0.03$ is favored from the “naturalness” point of view.

To understand better, the overall “naturalness” behaviour of the various parametrizations of the ERMF model presented in Table III, we consider the ratio of the largest to the smallest parameters for a given set. One expects this ratio to be of the order of unity if the parameters strictly obey the “naturalness”. We find that the ratio of the largest to the smallest parameters are 9.8, 8.0 and 220.1 for the FSUGZ00, FSUGZ03 and FSUGZ06 parametrizations,

respectively. Though, the FSUGZ03 parameter set is favoured from the “naturalness” point of view, it requires further improvement to obey the “naturalness” criteria in a more stringent manner. From the naturalness viewpoint, FUGZ03 parametrization can be improved by considering few additional terms in the energy density functional (Eq.(1)). Indeed, it is clear from the findings of Ref. [3] that the next higher order term containing gradients of the fields are necessary for the overall improvements of the “naturalness” behaviour of the parameters.

Before embarking on the discussion of our results, we would like to focus on the strong correlations existing between the parameters of the ERMF model which can be seen from Tables II and III. It is evident from Eqs. (13) - (22) that for given values of ϵ , K , M^* and ρ_0 , the coupling constants g_σ , g_ω , $\bar{\kappa}$ and $\bar{\lambda}$ are correlated with $\bar{\alpha}_1$, $\bar{\alpha}'_1$ and ζ . The value of ζ also affects the symmetry energy coefficient and its density dependence due to the mixed term containing ω and ρ meson fields. In other words, the coupling constants g_ρ and $\bar{\alpha}'_3$ are also correlated with ζ . So, it is very important to constrain the value of ζ . This can be achieved only if the behaviour of the EOS at higher densities or the maximum mass of the neutron stars are known. To constrain the values of $\bar{\alpha}_1$ and $\bar{\alpha}'_1$ one needs to know the density dependence of the effective meson masses. The values of $\bar{\alpha}_2$, $\bar{\alpha}'_2$ and $\bar{\alpha}'_3$ can be fixed by the neutron-skin thicknesses of asymmetric nuclei.

V. NUCLEAR AND NEUTRON MATTERS

In this section we discuss our results for the symmetric nuclear matter (SNM) and pure neutron matter (PNM). In Table IV we present our results for the various properties associated with the SNM at the saturation density. The quantity L in Table IV determines the linear density dependence of the symmetry energy coefficient J and is given by,

$$L = 3\rho \left. \frac{dJ}{d\rho} \right|_{\rho=\rho_0} \quad (24)$$

All the nuclear matter quantities given in the table for the FSUGZ and FSUGold parameters are more or less close to each other. The values of nuclear matter incompressibility coefficient, the symmetry energy coefficient and the linear density dependence of symmetry energy for the NL3 parameter set are much higher than that for our new parameter sets.

We use our newly generated parameter sets to study the effects of OMSC parameter ζ

on the EOS for the SNM and PNM. In Fig. 1 we plot the difference between the energy per nucleon $\Delta\epsilon = \epsilon(\zeta = 0) - \epsilon(\zeta)$ as a function of ζ for SNM(dotted lines) and PNM(solid lines) at fixed densities $\rho = 0.5 \text{ fm}^{-3}$ and 0.8 fm^{-3} . We calculate $\epsilon(\zeta)$ at $\zeta = 0.0, 0.01, \dots, 0.06$ using the parameter sets FSUGZ00, FSUGZ01, ..., FSUGZ06, respectively. We see that $\Delta\epsilon$ increases with increase in ζ . In other words, the $\epsilon(\zeta)$ decreases with increase in ζ implying that EOS becomes softer as ζ increases. At higher densities the values of ϵ appears to be very much sensitive to the value of ζ . For example, the value of $\Delta\epsilon$ at $\zeta = 0.06$ is less than 0.1 MeV for $\rho = 0.2 \text{ fm}^{-3}$ and it becomes greater than 125 MeV for $\rho = 0.8 \text{ fm}^{-3}$. It must be pointed once again, for different values of ζ the remaining parameters of the ERMF models are so adjusted that they appropriately fit the properties of the finite nuclei. We find that FSUGZ03 parametrization which corresponds to a moderate value of ζ yields an EOS which is neither too stiff nor too soft. In Figs. 2(a) and 2(b) we plot the EOS for SNM and PNM obtained using FSUGZ03 parametrization which agree reasonably well with the EOS obtained within the DBHF framework [27]. The NL3 and FSUGold parametrizations yield the EOS which show larger deviations, in particular, at higher densities as compare to the DBHF results. The NL3 parameters gives very stiff EOS while the FSUGold parameters gives rise to very soft EOS.

VI. FINITE NUCLEI

The fit to the properties of the finite nuclei for the parameter sets FSUGZ00 - FSUGZ06 are very much similar. For the sake of clarity we present our results obtained for the finite nuclei only for the parameter set FSUGZ03. In Fig.3 we display the values of the relative error in the total binding energies $\delta B = (B^{exp} - B^{th})/B^{exp}$ in percent obtained for the FSUGZ03 parametrization. For the comparison, we also display the similar results obtained for the NL3 and FSUGold parameter sets. It is clear that the binding energies obtained using FSUGZ03 parameter set agree better with the experimental data than those for the NL3 and FSUGold parameter sets. The rms errors in the total binding energies are 1.6, 2.5 and 3.6 MeV calculated using FSUGZ03, NL3 and FSUGold parameter sets, respectively. For other FSUGZ parameter sets the rms errors in the total binding energies lie in between 1.5 – 1.8 MeV. In Fig. 4 we display our results for the relative error δr_{ch} in percent for the charge rms radii and compare them with the ones obtained for the NL3 and FSUGold

parametrizations. The values of charge rms radii calculated for various parametrizations differ only marginally. The rms errors in the charge rms radii are 0.03, 0.02 and 0.03 fm for the FSUGZ03, NL3 and FSUGold parameter sets, respectively. Our results for the neutron-skin thickness $\Delta r = r_n - r_p$ are plotted in Fig. 5. The values of the rms radii r_n and r_p are calculated using the point density distributions for neutrons and protons, respectively. The values of Δr shown by crosses are the predictions based upon the DBHF calculations [25] and isospin diffusion data [26]. We see that the values of Δr obtained using FSUGZ03 and that for the FSUGold parameter sets are closer to the predicted values. The NL3 parameters significantly overestimates the values of Δr . We would like to mention here that for the NL3 type of parametrization the values of the symmetry energy coefficient J and its linear density dependent L are determined by a single parameter g_ρ which determines the coupling of ρ mesons with the nucleons. It may be therefore not possible with NL3 type of parametrization to fit simultaneously the values of the binding energies and the neutron-skin thicknesses for asymmetric nuclei. However, in the ERMF model, the mixed interactions of σ and ω mesons with the ρ mesons makes it possible to give a wide spread in the values of neutron-skin thicknesses without affecting the other properties of finite nuclei [28, 29].

VII. NEUTRON STARS

In Sec. V we have seen that the energy per nucleon decreases as the OMSC parameter ζ increases (see Fig.1). This effect is more pronounced at higher densities which implies that as ζ increases the EOS at higher densities becomes softer. Thus, it is natural to expect the differences in the properties of the neutron stars obtained for our new parameter sets with different values of OMSC. In this section we present our results for the properties of the neutron stars obtained for the seven different parameter sets FSUGZ00 – FSUGZ06. The neutron star properties we have considered are the limiting mass, central density and radius for the neutron star with the “canonical” mass of $1.4M_\odot$. These properties are determined by integrating the Tolman-Oppenheimer-Volkoff (TOV) equations [30]. The TOV equations are solved using EOS for the matter consisting of neutrons, protons, electrons and muons. The composition of matter at any density is so determined that charge neutrality and β -equilibrium conditions are satisfied. For densities higher than 0.08 fm^{-3} , the nuclear part of EOS is evaluated within the ERMF model and that for electrons and muons the Fermi gas

approximation is used. At densities lower than 0.08 fm^{-3} down to $6.0 \times 10^{-12} \text{ fm}^{-3}$ we use the EOS of Baym-Pethick-Sutherland [31].

In Fig. 6 we plot mass-radius relationship for the neutron stars calculated using FSUGZ00, FSUGZ03 and FSUGZ06 parametrizations. For the sake of comparison we also plot the similar results obtained using FSUGold and NL3 parameter sets. The region bounded by $R \leq 3GM/c^2$ is excluded by the causality limit [32]. The line labeled by $\Delta I/I = 0.014$ is radius limit estimated by Vela pulsar glitches [33]. The rotation constraint as indicated in Fig. 6 is obtained using [34],

$$\nu_k = 1045 \left(\frac{M}{M_\odot} \right)^{1/2} \left(\frac{10 \text{ km}}{R} \right)^{3/2} \text{ Hz} \quad (25)$$

where, the frequency ν_k is taken to be 641 Hz which is the highest observed spin rate from the pulsar PSR B1937+21. We see from Fig. 6 that as the mass of the neutron stars increases, the radius show stronger ζ dependence. In particular, radius for the $1.4M_\odot$ neutron stars decreases linearly from 13.2 Km at $\zeta = 0.0$ to 12.4 Km at $\zeta = 0.06$. We also calculate the radiation radius,

$$R_\infty = \frac{R}{\sqrt{1 - \frac{2GM}{Rc^2}}} \quad (26)$$

for the neutron with the canonical mass $1.4M_\odot$. For our parameter sets, R_∞ lies in the range of 15.19 – 15.93 km.

In Fig.7 we have plotted the variation of the limiting mass M_{max} for the neutron stars as a function of OMSC parameter ζ . The ζ dependence of the various neutron star properties considered here are obtained using the parameter sets FSUGZ00 – FSUGZ06 for which ζ takes the values 0.0 – 0.06, respectively. The remaining parameters for the FSUGZ sets are adjusted to fit the properties of the finite nuclei. The symbols open circle and square at $\zeta = 0.0$ and 0.06 represent the values of the limiting mass for the NL3 and FSUGold parametrizations, respectively. The value of M_{max} decreases with increase in ζ , because, with the increase in ζ the EOS becomes softer. It is to be noted that the NL3 and FSUGZ00 parametrizations have $\zeta = 0$. The only difference is that the FSUGZ00 parameter set contains additional contributions from the mixed interactions between σ , ω and ρ mesons and values of K, J and L are much smaller. The value of M_{max} for FSUGold and FSUGZ06 parameter sets are vary close, since, both these parameter sets have $\zeta = 0.06$ and have similar nuclear matter properties. For our case the M_{max} varies between $2.3M_\odot - 1.7M_\odot$

for $0 \leq \zeta \leq 0.06$. For the similar range of ζ , the calculations performed in Ref.[6] yield the M_{max} varying between $2.8M_\odot - 1.8M_\odot$ which is significantly larger. The value of M_{max} in Ref.[6] is obtained without including the contributions from the mixed interactions. Unlike, in our case, the parameter sets for different values of OMSC used in Ref.[6] are generated without constraining the value of L as given by Eq.(24). We must also point out that for moderate values of OMSC ($\zeta \sim 0.03$) we get $M_{max} \sim 1.9 M_\odot$. In the present work we do not consider the influence of the self-coupling of the ρ mesons on the maximum mass of the neutron stars. It is shown in Ref. [6] that when the ρ meson self-coupling is varied within the bounds of the “naturalness”, the maximum mass of the neutron star composed of the β -equilibrated matter can increase at most by $0.1M_\odot$.

In Fig. 8 we plot our results for the proton fractions as a function of baryon density. The solid circles represent the threshold density at which the condition [35],

$$Y_n^{1/3} \leq Y_p^{1/3} + Y_e^{1/3} \quad (27)$$

for the direct Urca (DU) process to occur is satisfied, where, $Y_i = \rho_i/\rho$ is the fraction for the i -th species. For the neutron star composed of neutrons, protons, electrons and muons, the critical value of the proton fraction Y_{DU} at which DU process sets in can be obtained from Eq. (27) together with the charge neutrality condition as,

$$Y_{DU} = \frac{1}{1 + \left[1 + \left(\frac{Y_e}{Y_e + Y_\mu} \right)^{1/3} \right]^3}. \quad (28)$$

It is clear from the Eq. (28) that at very low densities when $Y_\mu = 0$, Y_{DU} becomes 0.11. At extremely high densities when $Y_e \approx Y_\mu = \frac{1}{2}$, Y_{DU} becomes 0.15. From Fig. 8 we see that the critical proton fraction is ~ 0.13 . In Fig.9 we plot the variations of the densities ρ_U and ρ_c as a function of ζ , where, the ρ_U is the density at which the direct Urca process sets in and ρ_c denotes the central density for the neutron star with the “canonical” mass of $1.4M_\odot$. As expected, ρ_U and ρ_c increase with ζ . However, it is interesting to note that $\rho_U > \rho_c$ for smaller ζ and $\rho_U < \rho_c$ for $\zeta \gtrsim 0.02$. This means that the direct Urca process can occur in the neutron stars for the “canonical” mass of $1.4M_\odot$ only for $\zeta \gtrsim 0.02$. Also, one can infer from the Fig.9 that the minimum mass M_U for the neutron star in which direct Urca process can occur will decrease with ζ . In Fig. 10 we plot M_U versus ζ .

We have not considered the hyperonic degrees of freedom in our calculations. The EOS with nucleons, hyperons and leptons are softer than the one without hyperons [36]. The

stiffer is the EOS without hyperons, more is the softening effect when hyperons are included [37, 38]. Thus, the results obtained with smaller values of ζ will be affected more than the ones obtained for larger values of ζ . As a result, we expect that the variations in the maximum mass with ζ would certainly decrease. Further, in the presence of hyperons the threshold density for the direct Urca process will be pushed up.

VIII. CONCLUSIONS

The effects of OMSC on the properties of finite nuclei and neutron stars are investigated using a ERMF model which includes the contributions from all possible mixed interactions between the σ , ω and ρ mesons upto the quartic order. The simulated annealing method is implemented for minimizing the χ^2 function required to determine the best fit parameters. For a realistic investigation, we generate seven different parameter sets named FSUGZ00, FSUGZ01,....., FSUGZ06 for different values of OMSC by adjusting the remaining parameters of the model to fit the properties of the finite nuclei. The properties of finite nuclei used in the fits are the total binding energies and charge rms radii for several closed shell nuclei ranging from normal to exotic ones. In addition, we also include in our fit neutron-skin thickness for ^{208}Pb nucleus to constrain the density dependence of the symmetry energy coefficient. The value of neutron-skin thickness is so chosen that it agrees reasonably well with the recent predictions [24, 25, 26]. All these parameter sets fit equally well the finite nuclear properties. But, only moderate values of OMSC are favored from the “naturalness” point of view. For our parameter sets the rms errors in the total binding energies calculated for the nuclei used in the fits are 1.5 – 1.8 MeV which are significantly smaller than 3.6 MeV obtained for recently proposed FSUGold parametrization.

The behaviour of EOS at higher densities is predominantly determined by the OMSC which is different for our different parameter sets. The parameter sets with moderate values of the OMSC not only exhibit the “naturalness”, but, also yield the EOS for the symmetric nuclear and pure neutron matters which closely resemble the ones calculated within the framework of the Dirac-Brueckner- Hartree-Fock. For such parameter sets the values of the limiting mass for the neutron stars is $\sim 1.9M_{\odot}$. For our various parametrizations the value of the limiting mass of the neutrons stars lie in the range of $1.7M_{\odot} - 2.3M_{\odot}$. We also find that the direct Urca process can occur in the neutron stars with “canonical” mass of $1.4M_{\odot}$ only for the moderate and higher values of OMSC. For our various parametrizations, the radius of $1.4M_{\odot}$ neutron stars lie in the range of 12.4 - 13.2 Km.

Acknowledgments

This work was supported in part by the University Grant Commission under grant # F.17-40/98 (SA-I).

-
- [1] R. Furnstahl, B. D. Serot, and H.-B. Tang, Nucl. Phys. **A598**, 539 (1996).
 - [2] B. D. Serot and J. D. Walecka, Int. J. Mod. Phys. E **6**, 515 (1997).
 - [3] R. Furnstahl, B. D. Serot, and H.-B. Tang, Nucl. Phys. **A615**, 441 (1997).
 - [4] J. D. Walecka, Ann. Phys. (N.Y.) **83**, 491 (1974).
 - [5] J. Boguta and A. R. Bodmer, Nucl. Phys. **A292**, 413 (1977).
 - [6] H. Müller and B. D. Serot, Nucl. Phys. **A606**, 508 (1996).
 - [7] M. D. Estal, M. Centelles, X. Vias, and S. K. Patra, Phys. Rev. C **63**, 024314 (2001).
 - [8] B. G. Todd-Rutel and J. Piekarewicz, Phys. Rev. Lett **95**, 122501 (2005).
 - [9] J. Piekarewicz and S. P. Weppner, nucl-th/0509019 (2005).
 - [10] N. K. Glendenning and S. A. Moszkowski, Phys. Rev. Lett. **67**, 2414 (1991).
 - [11] S. F. Ban, J. Li, S. Q. Zhang, H. Y. Jia, J. P. Sang, and J. Meng, Phys. Rev. C **69**, 045805 (2004).
 - [12] B. K. Agrawal, S. Shlomo, and V. K. Au, Phys. Rev. C **72**, 014310 (2005).
 - [13] B. K. Agrawal, S. K. Dhiman, and R. Kumar, Phys. Rev. C **73**, 034319 (2006).
 - [14] G. A. Lalazissis, J. König, and P. Ring, Phys. Rev. C **55**, 540 (1997).
 - [15] S. Kirkpatrik, J. Stat. Phys. **34**, 975 (1984).
 - [16] L. Ingber, Mathl. Comput. Modelling **12**, 967 (1989).
 - [17] B. Cohen, Master's thesis, Tel-Aviv University (1994).
 - [18] T. Bürvenich, D. G. Madland, J. A. Maruhn, and P.-G. Reinhard, Phys. Rev. C **65**, 044308 (2002).
 - [19] T. Bürvenich, D. G. Madland, and P.-G. Reinhard, Nucl. Phys. **A744**, 92 (2004).
 - [20] A. R. Bodmer, Nucl. Phys. **A526**, 703 (1991).
 - [21] G. Audi, A. H. Wapstra, and C. Thibault, Nucl. Phys. **A729**, 337 (2003).
 - [22] E. W. Otten, in *Treatise on Heavy-Ion Science*, vol. 8 (ed. D. A. Bromley, Plenum, New York, 1989).
 - [23] H. D. Vries, C. W. D. Jager, and C. D. Vries, At. Data Nucl. Data Tables **36**, 495 (1987).
 - [24] J. Piekarewicz, Phys. Rev. C **69**, 041301 (2004).
 - [25] D. Alonso and F. Sammarruca, Phys. Rev. C **68**, 054305 (2003).
 - [26] L.-W. Chen, C. M. Ko, and B.-A. Li, Phys. Rev. C **72**, 064309 (2005).

- [27] G. Q. Li, R. Machleidt, and R. Brockmann, Phys. Rev. C **45**, 2782 (1992).
- [28] R. Furnstahl, Nucl. Phys. **A706**, 85 (2002).
- [29] T. Sil, M. Centelles, X. Vinas, and J. Piekarewicz, Phys. Rev. **C71**, 045502 (2005).
- [30] S. Weinberg, *Gravitation and cosmology* (Wiley, New York, 1972).
- [31] G. Baym, C. Pethick, and P. Sutherland, Astrophys. J. **170**, 299 (1971).
- [32] J. M. Lattimer, M. Prakash, D. Masak, and A. Yahil, Astrophys. J. **355**, 241 (1990).
- [33] J. M. Lattimer and M. Prakash, Astrophys. J. **550**, 426 (2001).
- [34] J. M. Lattimer and M. Prakash, Science **304**, 536 (2004).
- [35] J. M. Lattimer, C. J. Pethick, M. Prakash, and P. Haensel, Phys. Rev. Lett. **66**, 2701 (1991).
- [36] N. Glendenning, *Compact Stars: Nuclear Physics, Particle Physics, and General Relativity* (Springer, New York, 2000).
- [37] S. Balberg, I. Lichtenstadt, and G. B. Cook, Astrophys. J. **S121**, 515 (1999).
- [38] H. J. Schulze, A. Polls, A. Ramos, and I. Vidana, Phys. Rev. C **73**, 058801 (2006).

TABLE I: The lower (\mathbf{v}_0) and upper (\mathbf{v}_1) limits, maximum displacement (\mathbf{d}) and initial values (\mathbf{v}_{in}) for the ERMF model parameters used for minimizing the χ^2 value within the SAM. The nucleon, omega and rho masses are kept fixed at $M = 939$ MeV, $m_\omega = 782.5$ MeV and $m_\rho = 770$ MeV, respectively.

	\mathbf{v}_0	\mathbf{v}_1	\mathbf{d}	\mathbf{v}_{in}
$\epsilon(\text{MeV})$	-16.50	-15.50	0.1	-16.00
$K(\text{MeV})$	220.0	240.0	2.0	230.0
M^*/M	0.60	0.70	0.01	0.65
$\rho_0(\text{fm}^{-3})$	0.145	0.165	0.002	0.155
g_ρ	10.0	15.0	0.5	12.50
$\overline{\alpha}_1(\text{fm}^{-1})$	0.0	0.0095	0.0010	0.005
$\overline{\alpha}'_1$	0.0	0.0040	0.0004	0.002
$\overline{\alpha}_2(\text{fm}^{-1})$	0.0	0.0380	0.0038	0.019
$\overline{\alpha}'_2$	0.0	0.0160	0.0016	0.008
$\overline{\alpha}'_3$	0.0	0.0160	0.0016	0.008
$m_\sigma(\text{MeV})$	490.0	510.0	2.0	500.0

TABLE II: Various newly generated parameter sets FSUGZ00, FSUGZ03 and FSUGZ06 for the ERMF models. The parameters $\bar{\kappa}$, $\bar{\alpha}_1$, $\bar{\alpha}_2$ are given in units of fm^{-1} . The nucleon mass M and meson masses m_σ , m_ω and m_ρ are given in units of MeV. The parameters for the NL3 and FSUGold sets are taken from Refs. [8, 14]

Parameters	NL3	FSUGold	FSUGZ00	FSUGZ03	FSUGZ06
g_σ	10.21743	10.59217	10.65616	10.76145	11.02412
g_ω	12.86764	14.30207	13.95799	14.11104	14.66595
g_ρ	8.94880	11.76733	14.32687	14.67414	14.52185
$\bar{\kappa}$	0.019573	0.007194	0.030215	0.015606	0.006949
$\bar{\lambda}$	-0.015914	0.023762	-0.004544	0.009753	0.024487
ζ	—	0.060000	0.0	0.030000	0.060000
$\bar{\alpha}_1$	—	—	0.003867	0.001031	0.000045
$\bar{\alpha}'_1$	—	—	0.000779	0.000507	0.000053
$\bar{\alpha}_2$	—	—	0.029179	0.030682	0.025836
$\bar{\alpha}'_2$	—	—	0.013501	0.011625	0.015688
$\bar{\alpha}'_3$	—	0.600000	0.014759	0.013598	0.015849
M	939	939	939	939	939
m_σ	508.194	491.500	495.763	500.511	501.370
m_ω	782.501	782.500	782.500	782.500	782.500
m_ρ	763.0	763.0	770.0	770.0	770.0

TABLE III: The values of parameters expressed as dimensionless ratios using Eq.(11). All the values have been multiplied by 10^3

	NL3	FSUGold	FSUGZ00	FSUGZ03	FSUGZ06
$\frac{1}{2c_\sigma^2 M^2}$	1.403	1.221	1.227	1.227	1.173
$\frac{1}{2c_\omega^2 M^2}$	2.097	1.698	1.782	1.744	1.614
$\frac{1}{8c_\rho^2 M^2}$	1.030	0.596	0.409	0.390	0.399
$\frac{\bar{\kappa}}{6M}$	0.686	0.252	1.0508	0.547	0.243
$\frac{\bar{\lambda}}{24}$	-0.663	0.990	-0.189	0.406	1.020
$\frac{\zeta}{24}$	—	2.500	—	1.250	2.500
$\frac{\bar{\alpha}_1}{M}$	—	—	0.813	0.217	0.009
$\frac{\bar{\alpha}'_1}{2}$	—	—	0.389	0.253	0.026
$\frac{\bar{\alpha}_2}{4M}$	—	—	1.533	1.612	1.357
$\frac{\bar{\alpha}'_2}{8}$	—	—	1.688	1.453	1.961
$\frac{\bar{\alpha}'_3}{8}$	—	7.500	1.844	1.699	1.981

TABLE IV: The Nuclear matter properties at the saturation density for newly generated parameter sets FSUGZ00, FSUGZ03 and FSUGZ06 are compared with the corresponding ones obtained using NL3 and FSUGold parameter sets. The quantities given below are: ϵ the binding energy per nucleon, K the nuclear matter incompressibility coefficient, J the symmetry energy, $L = 3\rho \frac{dJ}{d\rho}$ related to the slope of the symmetry energy, M^*/M is the ratio of the effective nucleon mass to the nucleon mass and ρ_0 the saturation density.

	NL3	FSUGold	FSUGZ00	FSUGZ03	FSUGZ06
$\epsilon(\text{MeV})$	-16.25	-16.29	-16.03	-16.07	-16.05
$K(\text{MeV})$	271.5	230.0	240.0	232.5	224.9
$J(\text{MeV})$	37.40	32.59	31.43	31.55	31.17
$L(\text{MeV})$	118.56	60.56	62.19	64.01	62.43
M^*/M	0.595	0.609	0.605	0.603	0.607
$\rho_0(\text{fm}^{-3})$	0.148	0.148	0.149	0.147	0.146

FIG. 1: The difference between energy per nucleon $\Delta\epsilon = \epsilon(\zeta = 0) - \epsilon(\zeta)$ are plotted as a function of ζ for the SNM (dotted lines) and PNM (solid lines). The results for the $\epsilon(\zeta)$ are obtained for $\zeta = 0 - 0.06$ by using the parameter sets FSUGZ00 – FSUGZ06. The differences $\Delta\epsilon$ at higher densities are very sensitive to the value of ζ .

FIG. 2: The EOS for the (a) SNM and (b) PNM for the FSUGZ03 parametrization are compared with the ones calculated within the DBHF framework for a realistic potential [27]. Similar results for the NL3 and FSUGold parametrizations are also shown.

FIG. 3: Relative errors in the total binding energy $\delta B = (B^{exp} - B^{th})/B^{exp}$ for the newly generated parameter set FSUGZ03. For the sake of comparison, the values of δB obtained for NL3 and FSUGold parameter sets are also displayed. The rms errors in the total binding energies obtained by considering the nuclei used in our fits are 1.6, 2.5 and 3.6 MeV for the FSUGZ03, NL3 and FSUGold parameter sets, respectively.

FIG. 4: Relative errors in the charge rms radii δr_{ch} for the newly generated parameter set FSUGZ03. Similar results obtained using NL3 and FSUGold parameter sets are also plotted. The rms errors in the charge rms radii obtained by considering the nuclei used in our fits are 0.03, 0.02 and 0.03 fm for the FSUGZ03, NL3 and FSUGold parameter sets, respectively.

FIG. 5: Comparison of the results for the neutron-skin thickness $\Delta r = r_n - r_p$ obtained using the FSUGZ03, NL3 and FSUGold parameter sets. The crosses are the recent predictions for Δr based upon the DBHF calculations [25] and isospin diffusion data [26].

FIG. 6: Relation between the neutron star mass and its radius R for the FSUGZ00, FSUGZ03, FSUGZ06, FSUGold and NL3 parametrizations. The various constraints as indicated by causality, rotation and $\Delta I/I = 0.014$ are discussed in the text.

FIG. 7: Variation of the limiting mass M_{max} of the neutron star with the OMSC parameter ζ . For different values of ζ the remaining parameters of the ERMF model are adjusted to give best fit to the properties of the finite nuclei.

FIG. 8: Proton fractions as a function of density for the FSUGZ00, FSUGZ03, FSUGZ06, FSUGold and NL3 parametrizations. The solid circles indicate the threshold density for the direct Urca process.

FIG. 9: The density ρ_U at which direct Urca process sets in and the central density ρ_c for the neutron stars with $1.4M_\odot$ as a function of OMSC parameter ζ .

FIG. 10: The minimum value of the neutron star mass M_U in which direct Urca process occurs as a function OMSC parameter ζ .

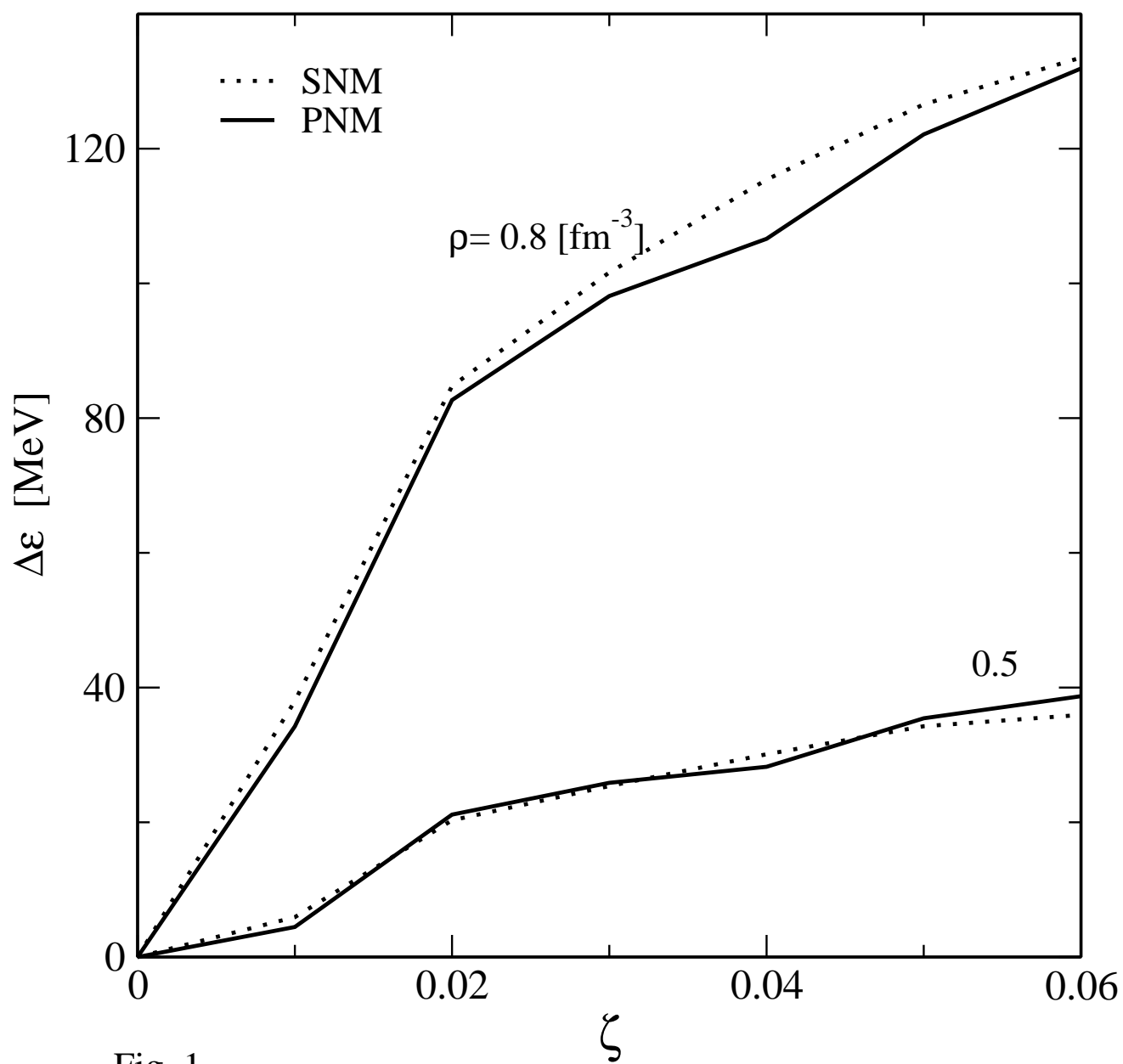


Fig. 1

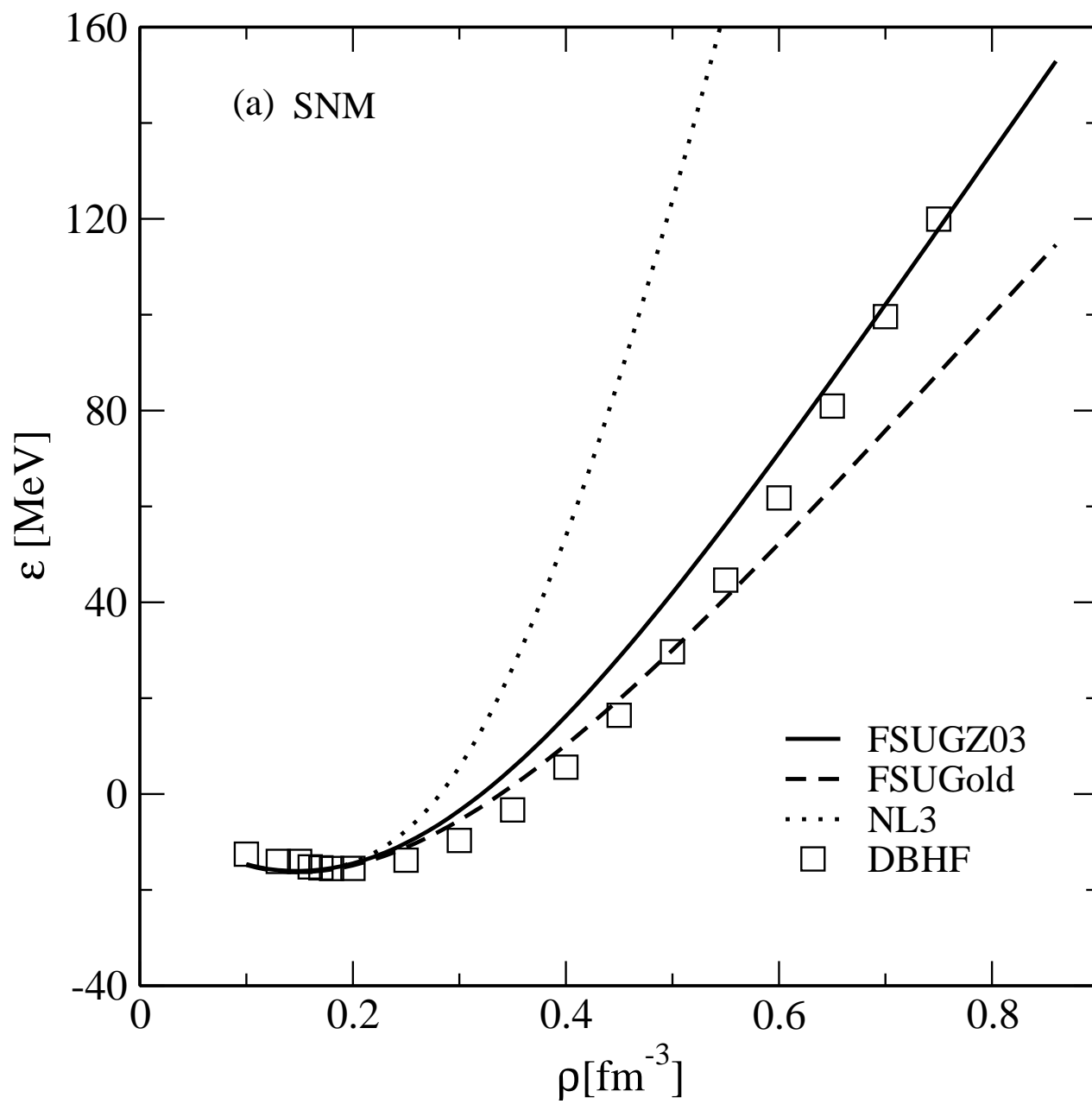


Fig. 2a

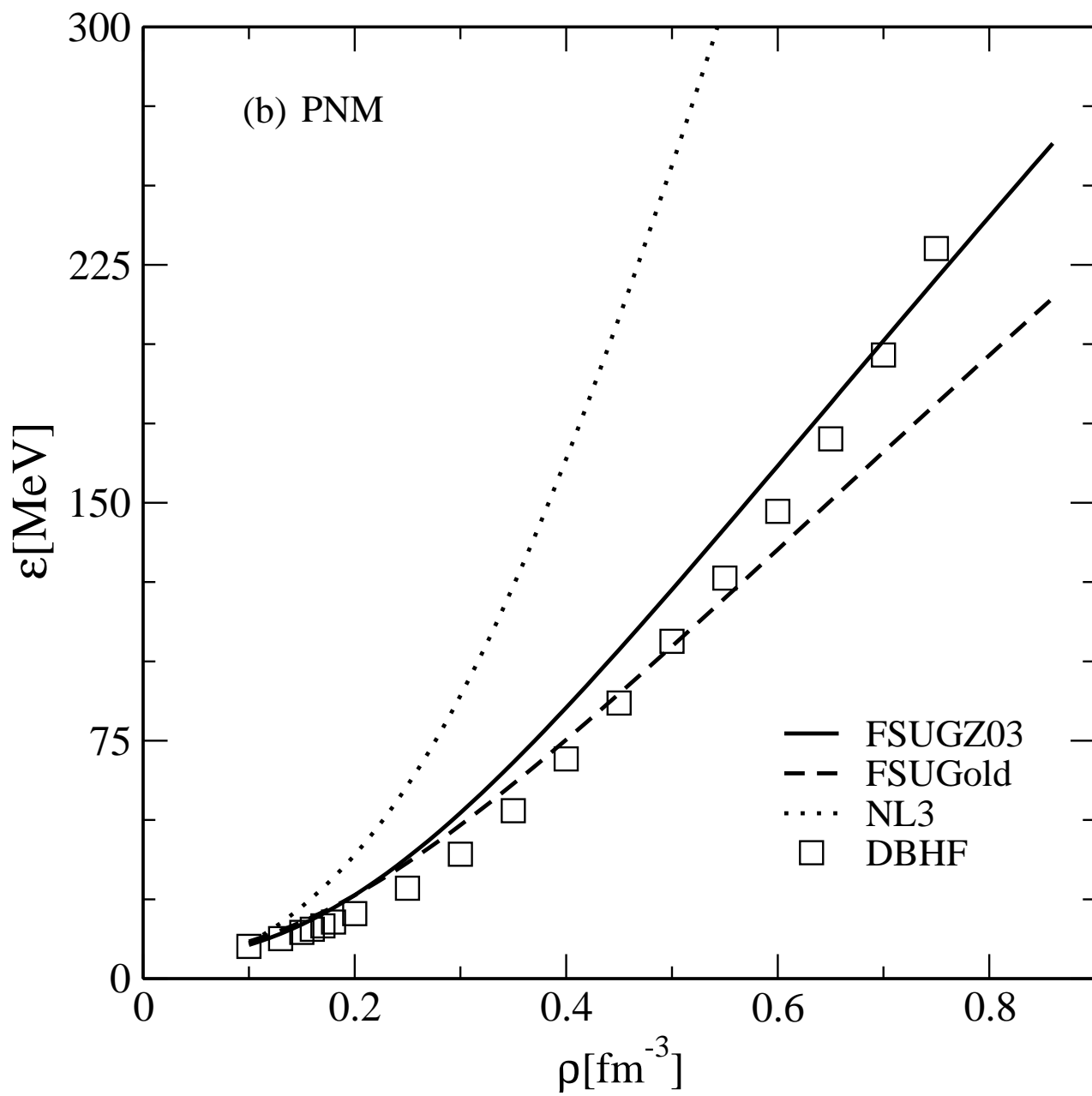


Fig. 2b

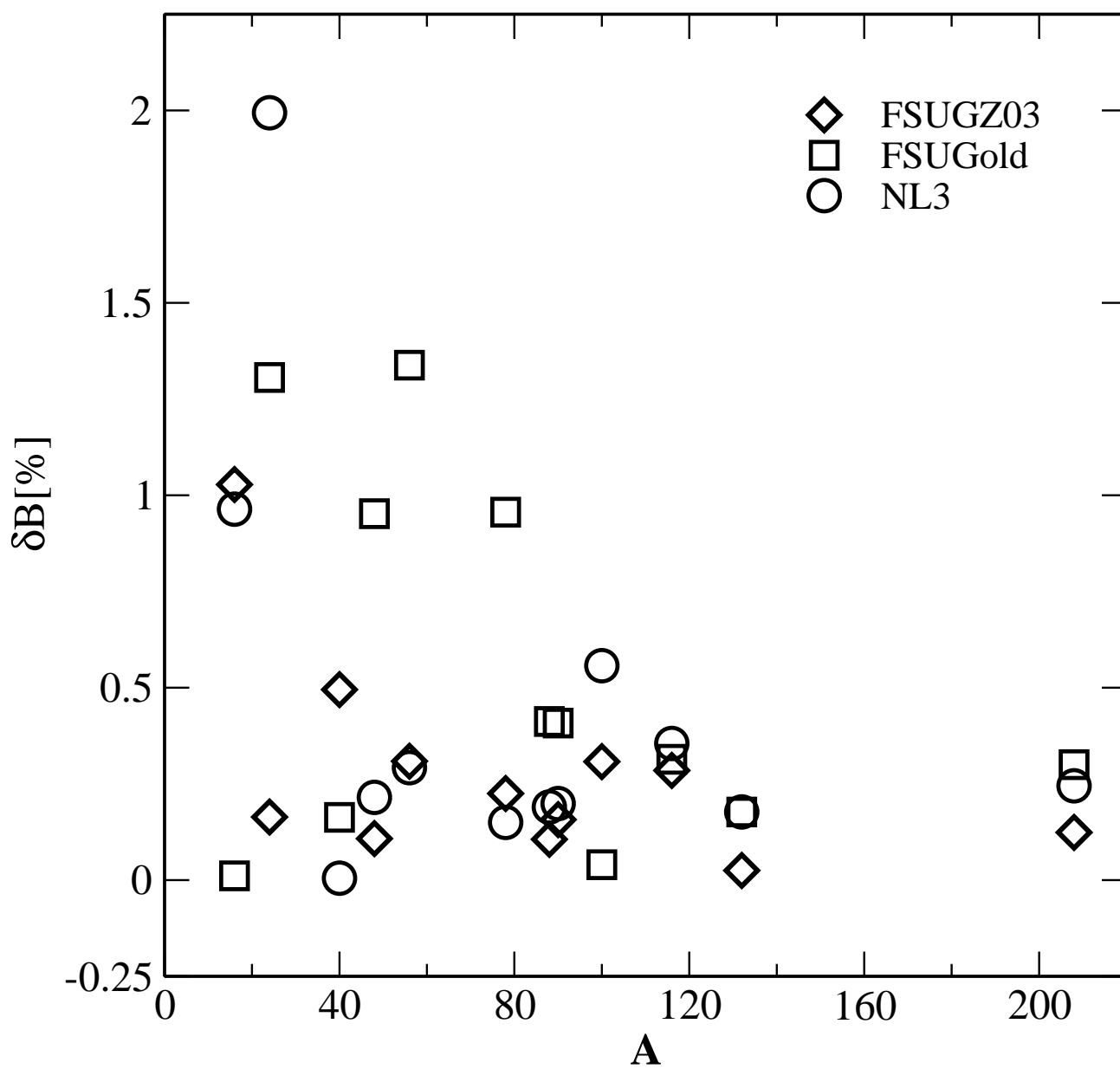


Fig. 3

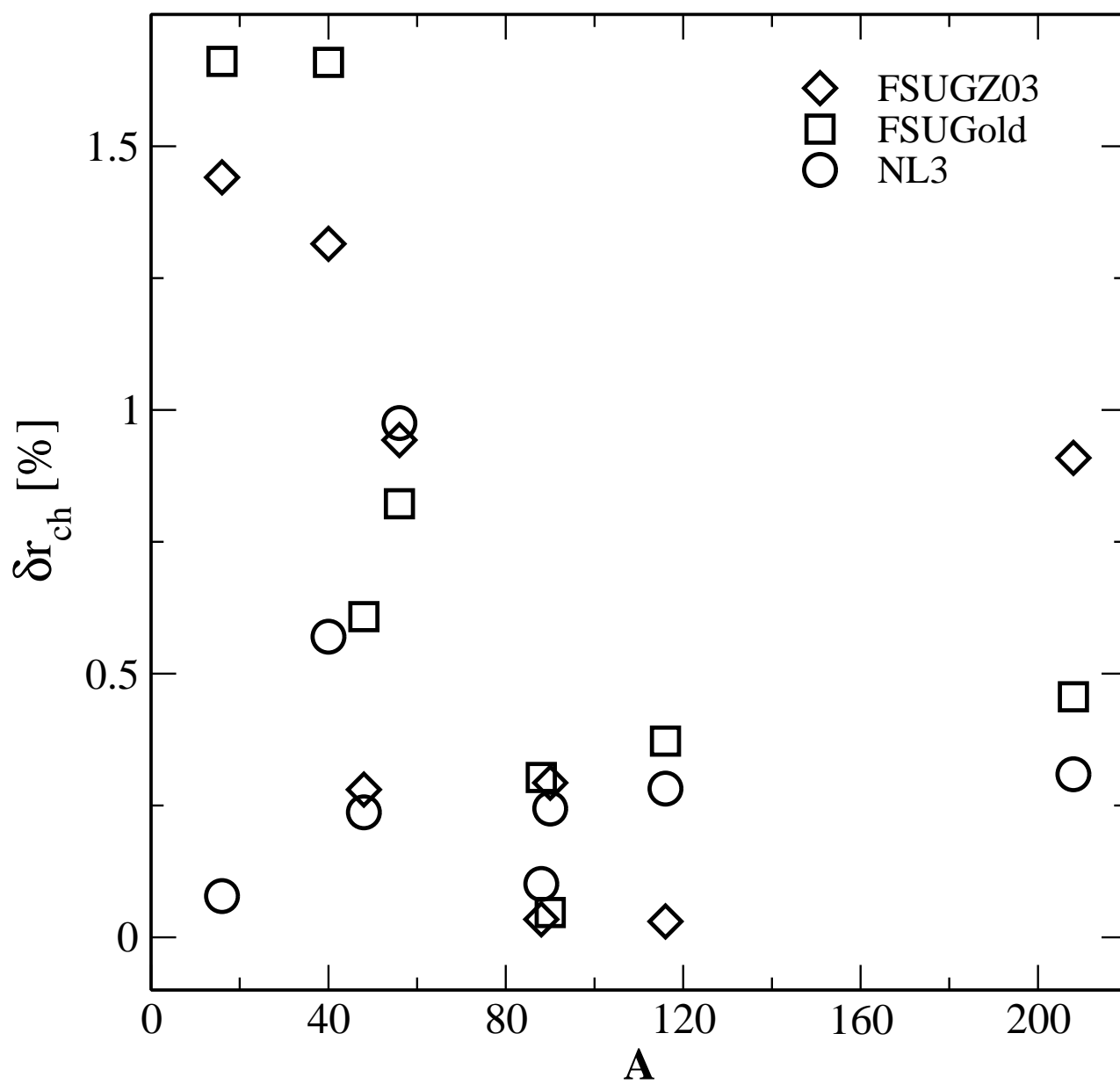


Fig.4

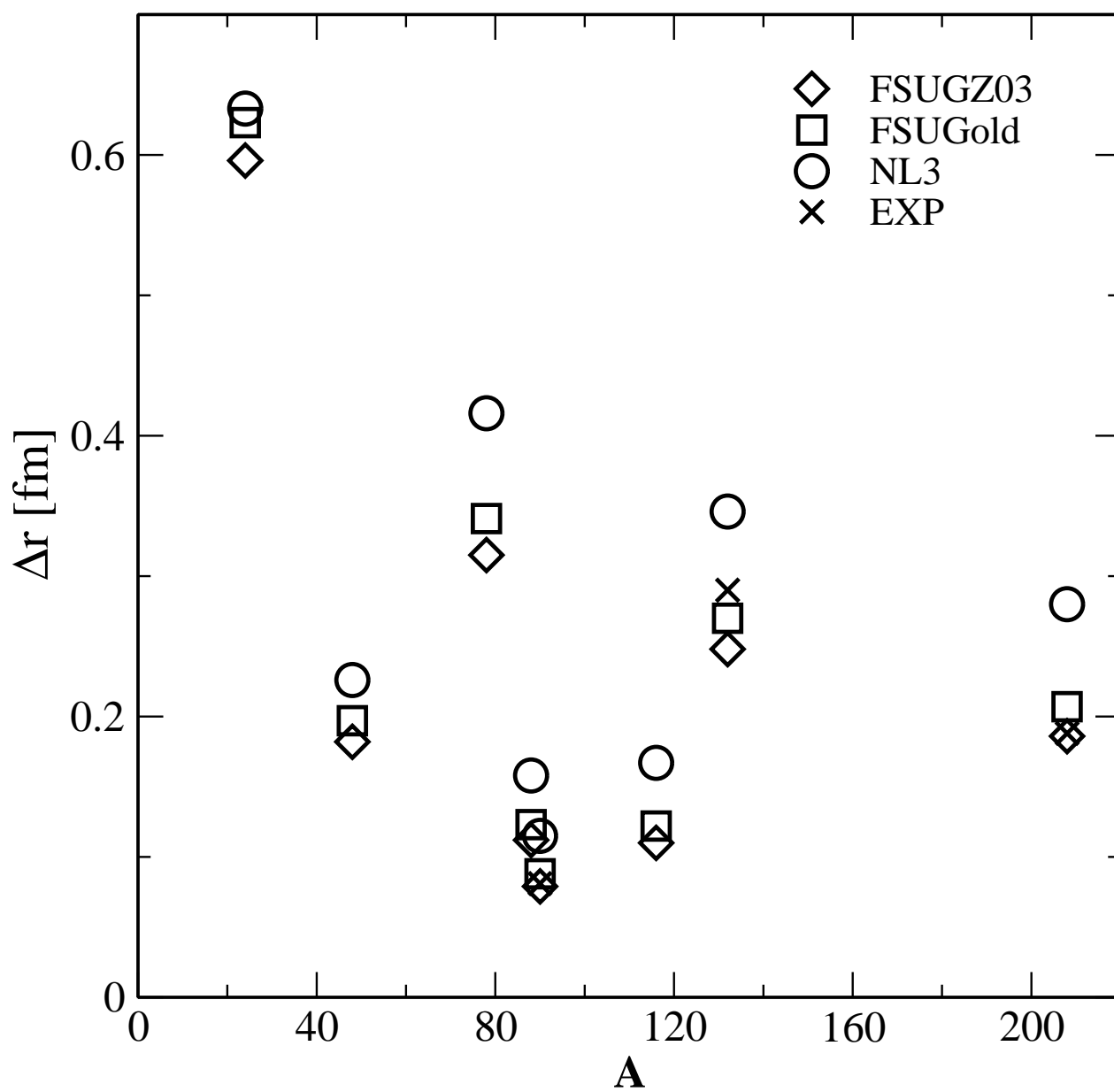


Fig. 5

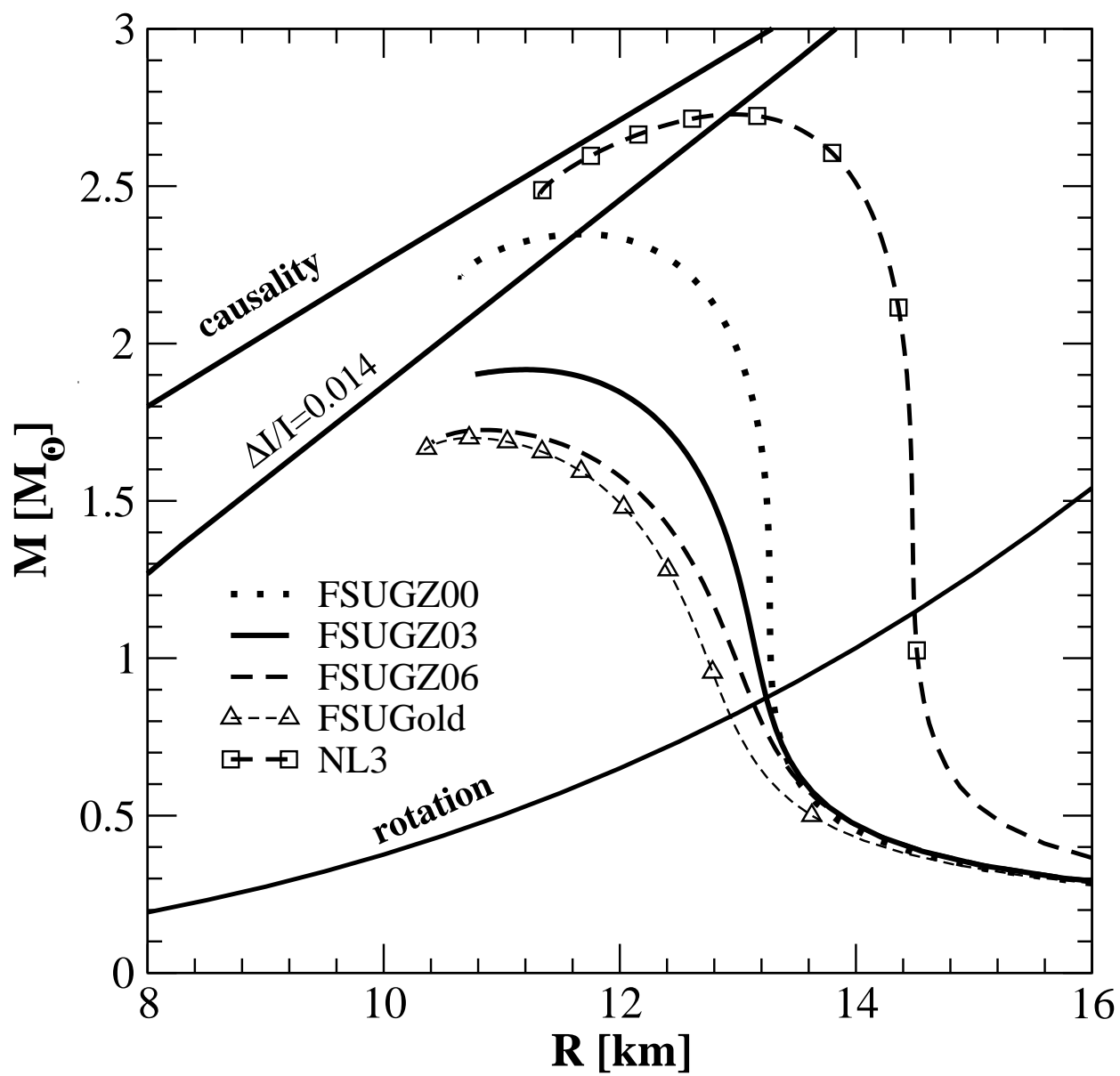


Fig. 6

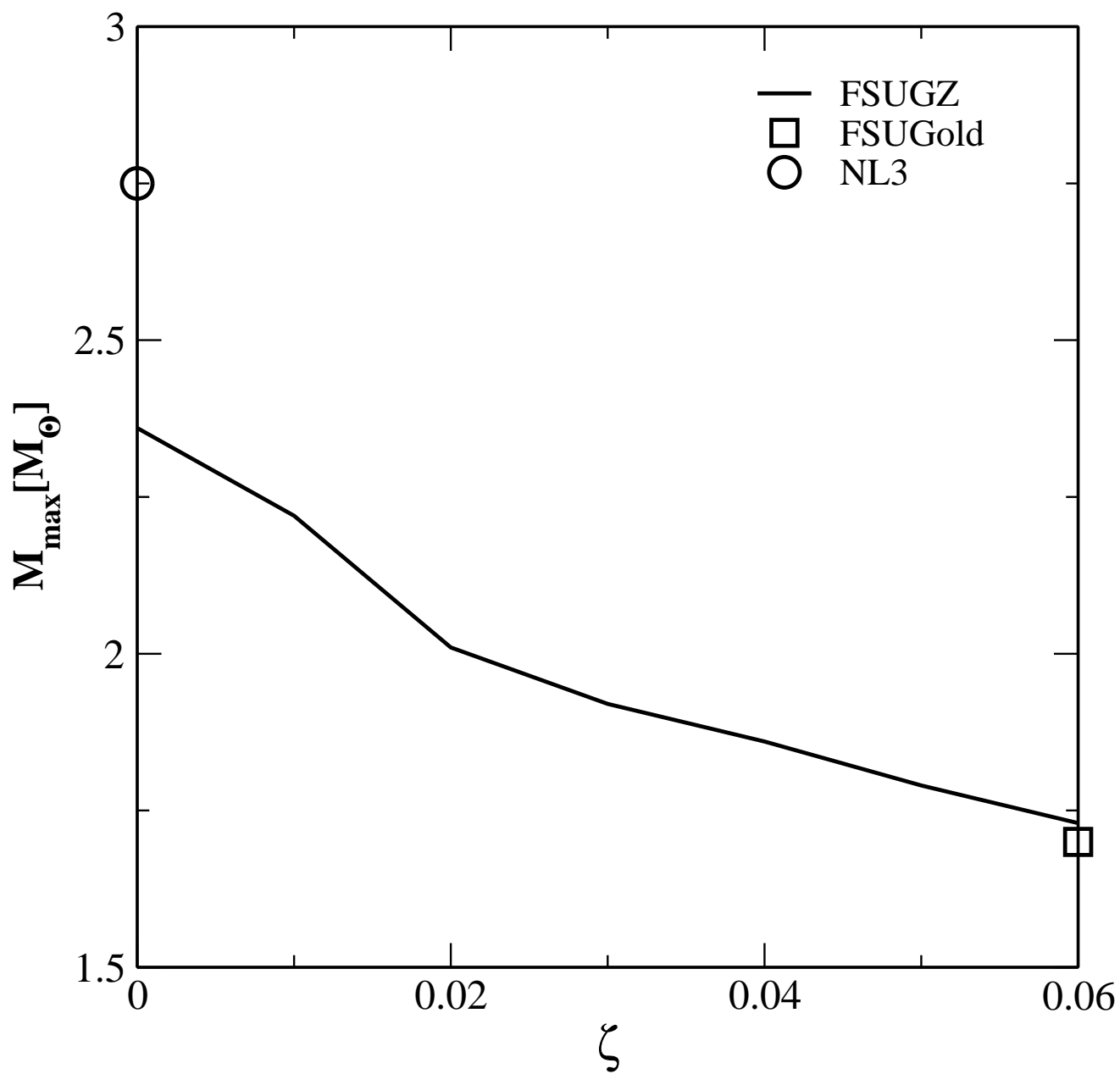


Fig. 7

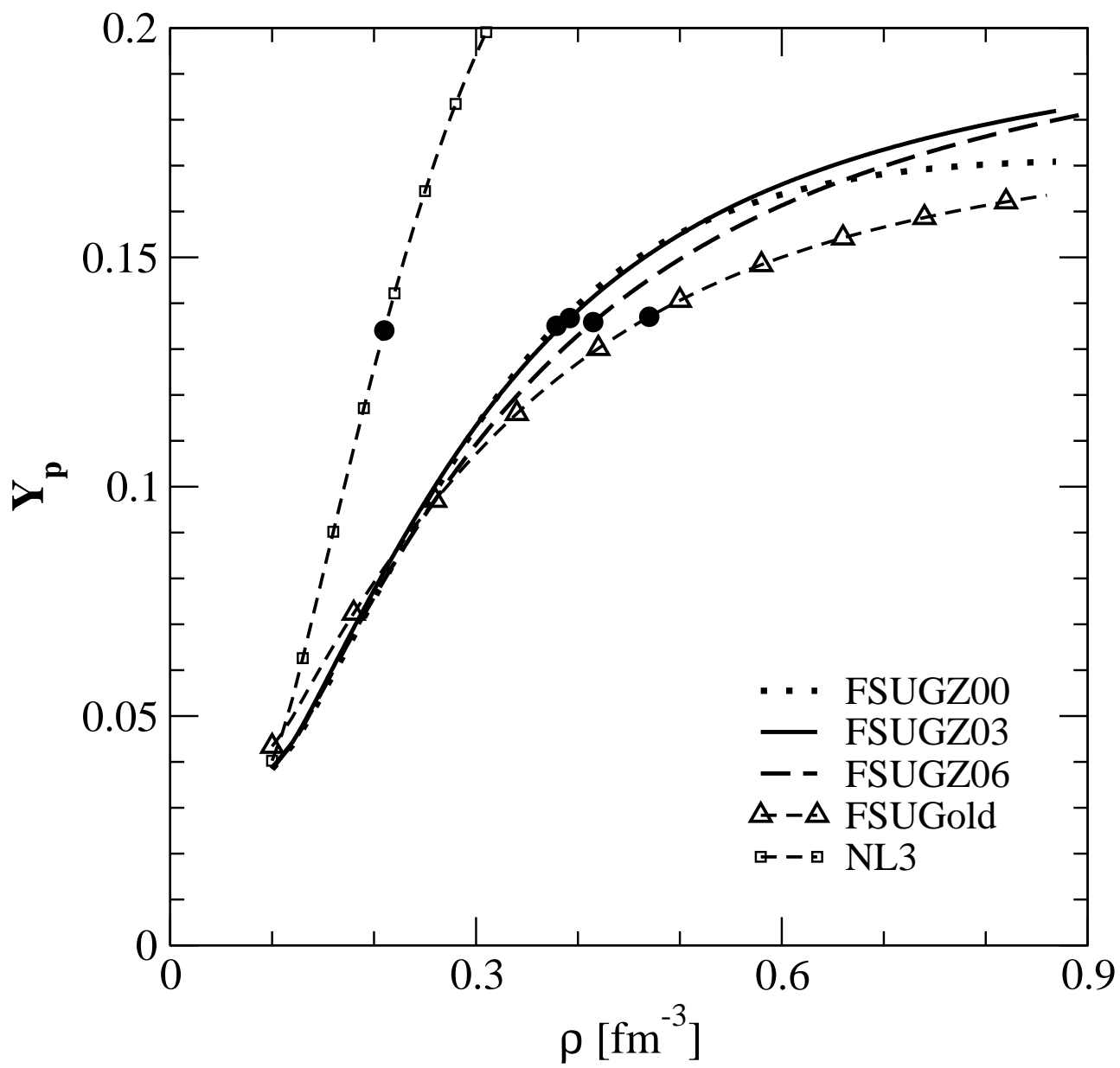


Fig. 8

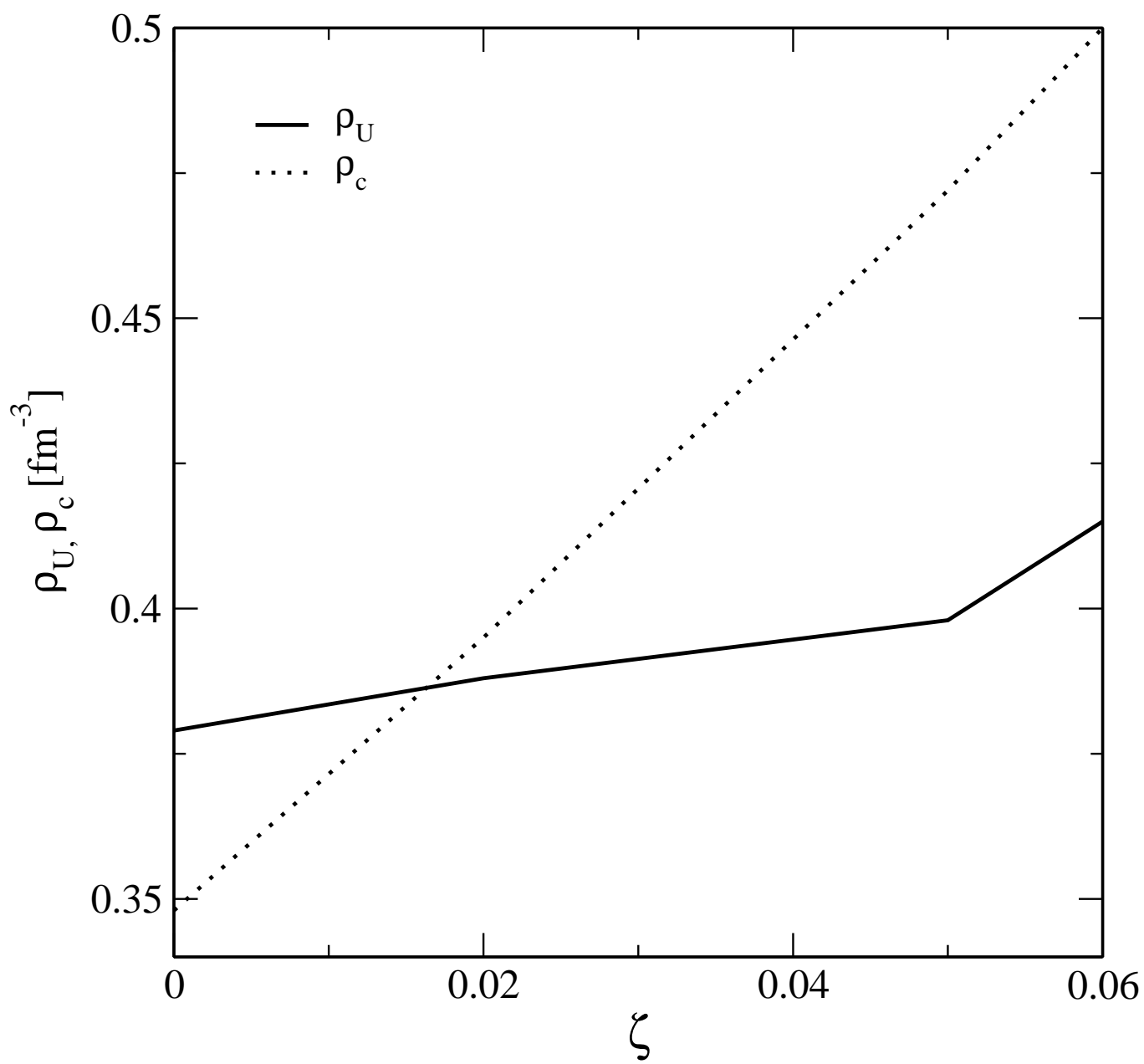


Fig. 9

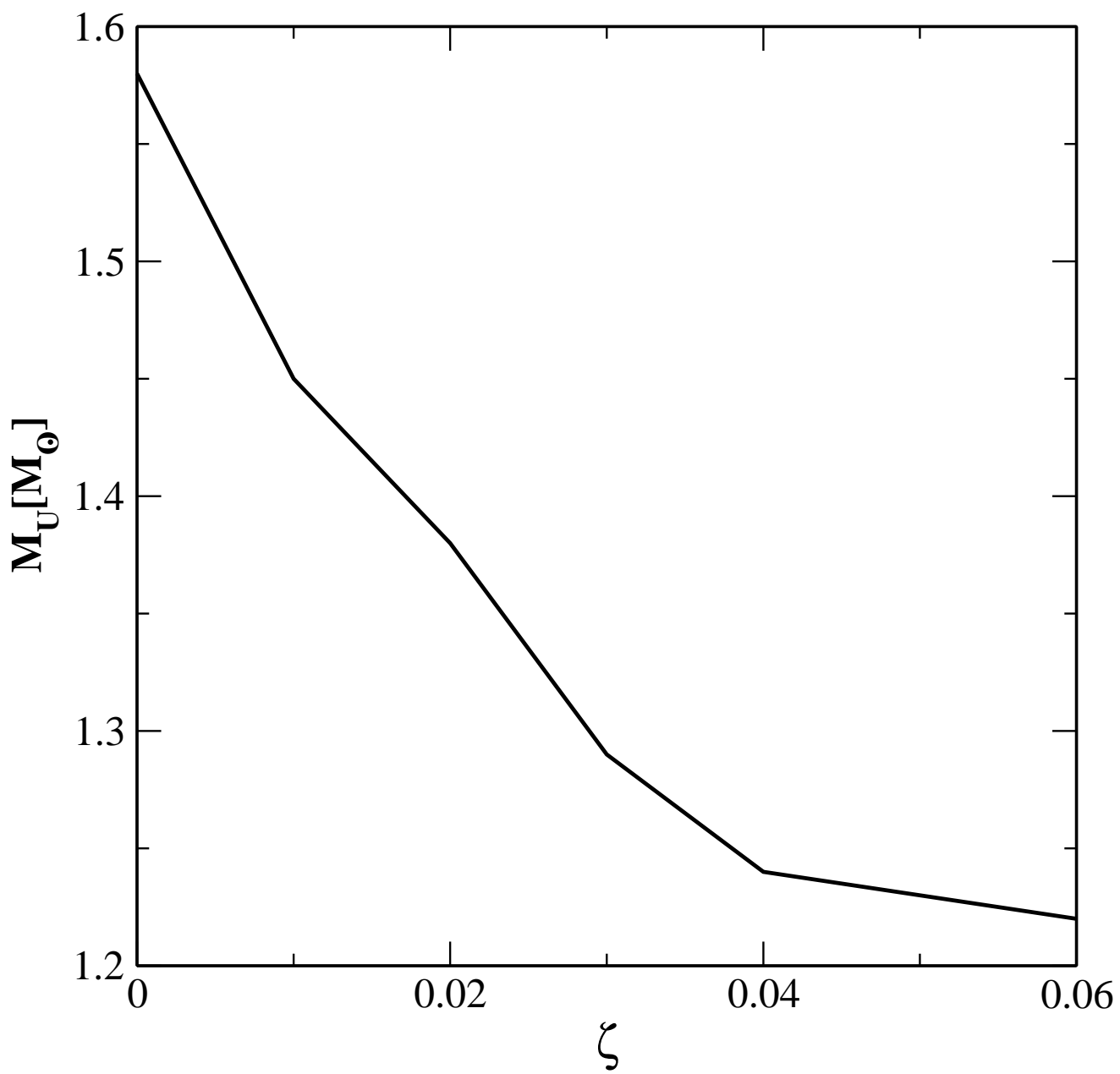


Fig. 10